International Journal of Geotechnical Earthquake Engineering
Volume 13 • Issue 1

Reliability-Based Fragility Analysis of RC Frame Buildings Considering Soil-Structure Interaction

Amit Shiuly, Jadavpur University, India*
https://orcid.org/0000-0002-4942-3042

Debapriya Das, Jadavpur University, India
https://orcid.org/0000-0001-8443-1577

ABSTRACT

In the present study, the effect of soil structure interaction (SSI) of low, mid, and high rise (G+1, G+4, and G+9 storey) buildings has been evaluated by nonlinear dynamic analysis using three-dimensional finite element method. Three types of uniform soils, namely hard soil, medium soil, and soft soil, have been considered for the present analysis. These buildings have been subjected to Loma Prieta (1989) earthquake motion and Denali (2002) earthquake motion as near field and far field earthquake motions respectively under the above mentioned soil conditions. From the analysis, the horizontal displacements and percentage of drifts have been determined of all the stories of the buildings under the above mentioned three soil conditions and the two earthquakes. Further, for all the cases, fragility curves have been computed. Furthermore, on the basis of the fragility curve and seismic hazard curve of a region, reliability index (RI) has also been developed.

KEYWORDS

Far Field Earthquake, Fragility Analysis, Near Field Earthquake, Reliability Index, Soil Condition, Soil Structure Interaction

1. INTRODUCTION

The characteristics of strong ground motion of an earthquake plays an important role on damage and destruction of structures. Soil play an important role in ground motion characteristics ((Nabilah et al., 2019) (Kumar et al., 2018) (Shiuly et al., 2014) (Kumar & Krishna, 2013) (Sitharam & Vipin, 2010) (Boominathan & Krishna Kumar, 2010)). Ground motion for a far source seismic event is ominously dissimilar than close source seismic event. It is to be noted that near source earthquake consists both high and low frequency seismic wave, whereas far source earthquake consists only low frequency

DOI: 10.4018/IJGEE.304911

*Corresponding Author

wave. Thus, respons of structure demonstrates amply difference for the two types of earthquake. It is to be mentioned that Soil Structure Interaction (SSI) effect is neglected in conventional earthquake analysis of structure. However, it has been observed that SSI plays an important role in variation of damage destructions of structures. On the basis of the type of soil and structure, the free-field response of a particular site may be amplified ominously due to SSI effect.

Several researches have conducted research on SSI effect in past. The procedure for determining the effects of inertial soil-structure interaction on structural response was demonstrated by Stewart et al. (1999). The effect of soil-structure interaction during the analysis and design of a six storeys RC frame building having basement was analysed by García (2008). Mylonakis et al. (2018) conducted research on the effect of SSI on the structural response subjected to earthquake motion and determined response spectrum specified in code along with amplified fundamental period and effective damping for the SSI. Anand et al (2010) defined the seismic behaviour of RC buildings with and without shear wall under various soil conditions incorporating SSI effect. The idealised 2-D finite element modelling of dynamic SSI assuming plane strain condition using Abaqus (v.6.8) software was performed by Matinmanesh et al. (2011). Priyanka et al. (2012) evaluated the effect of SSI on multi-storeyed buildings having various foundation systems. The dynamic behaviour of building frames on raft footing under seismic excitations incorporating the SSI effect was investigated by Kuladeepu et al. (2015). Gaikwad et al. (2015) investigated the effect of bare frames and in-filled frames considering effect of soil under seismic excitation. Several researchers conducted researches on the SSI effect due to far field and near field seismic event. Ghannad et al. (2008) explored the seismic response with SSI based on the concept of cone models subjected to near fault ground motions. Zhang and Tang (2008) conducted numerical modelling dynamic SSI by a lumped two degree of freedom system which was subjected to pulse like near fault ground excitation. A parametric study was performed by Azarhoosh and Ghodrati Amiri (2010) considering the elastic response of different SSI systems having shallow foundations and exposed to synthetic pulses and near fault excitations. Minasidis et al. (2014) inspected SSI effect of the response of 2D steel frames subjected to near fault earthquake excitation. Gelagoti et al. (2012) studied the seismic performance of rocking isolated frame structures considering SSI by employing nonlinear FEM. In this study near source ground motion was used to determine factor of safety against toppling collapse of the structure. Davoodi and Sadjadi (2012) evaluated response of single degree of freedom (SDOF) system with considering SSI subjected to near field and far field ground motion. the useful effect of allowing soil and structure uncertainties of different parameter on the soil-structure response was discussed by (2018).

Past literature corroborates that a lot of researches has been conducted on the seismic fragility analysis of structure. Singhal and Kiremidjian (1996) used LHS-Monte Carlo method for probabilistic evaluation of seismic structural damage and evaluated fragility curves for low, mid and high-rise RC buildings. Mosalam et al. (1997) conducted push over analysis on seismic fragility of Lightly Reinforced Concrete (LRC) frames with and without masonry infill walls. Guneyisi and Altay (2008) evaluated fragility curves for a RC office building retrofitted with fluid viscous dampers situated in Istanbul region. Suraj V. Borele (2015) explored the methodology for generating a fragility curve according to HAZUS technical manual. Reliability based seismic analysis and design of open ground storey frame buildings was conducted out by Pragalath (2016). Vazurkar and Chaudhari (2016) executed the vulnerability assessment of RC buildings using fragility curves. Further, several researchers performed reliability based assessment of structures using the fragility curves. Collins et al. (1996) explored dual-level seismic design which is a reliability-based methodology. Ellingwood (2001) discussed the significance of reliability analysis of building responses to understand the behaviour of buildings. Wen (2001) elaborated the concept of reliability and performance-based design.

The literature review clearly depicts that the reliability based fragility analysis under near field and far field ground motion on different types of buildings situated on different types of soil by considering soil structure interaction were not conducted by any researcher. In the present study an attempt has been made to fill the research gap by nonlinear dynamic analysis using three-dimensional finite element method software. Three types of uniform soils namely hard soil, medium soil and soft soil for low mid and high rise buildings (G+1, G+4 and G+9 storey) have been considered for the present investigation. The buildings under the above mentioned soil conditions have been subjected to Loma Prieta (1989) earthquake motion and Denali (2002) earthquake motion as near field and far field earthquake motions respectively. The horizontal displacements and percentage drifts of all the storeys of the buildings have been determined and fragility curves have been generated. In addition to that, on the basis of the fragility curve and seismic hazard curve of a region, RI have also been developed. The several important findings have been obtained from the present study.

2. PROBLEM FORMULATION

In this paper, an investigation has been made to observe the effect of various properties of soil and structure on dynamic SSI. To detect the effect of soil properties on dynamic SSI, three types of uniform soils (Hard Soil, Medium Soil and Soft Soil) have been considered here. It is assumed that all the soils are homogenous in nature. The mass density, Young's modulus and shear wave velocity in the soil medium are maximum for the hard soil and minimum for the soft one. On the other hand, Poisson's ratio is minimum for the hard soil and maximum for the soft soil. All the values for the medium soil lie between the hard and soft soil. However, the properties of all the soils used for developing the models have been presented in Table 1.

Further, to study the contribution of various structural properties towards dynamic SSI phenomenon, three frame buildings (G+1, G+4 and G+9) have been taken for analysis. All the buildings are square shaped having a plan dimension of 15 m × 15 m. Each building has three bays of same length in both the directions. The building heights have been taken as 6 m, 15 m and 30 m for the G+1, G+4 and G+9 building respectively. Floor to floor height of all the buildings is considered 3 m. As the foundation of the buildings, raft footings have been used. Various properties of the constituents of the buildings are shown in Table 2.

3. MODELLING THE PROBLEM

To model and analyse the dynamic SSI phenomenon, various techniques are followed. Among them, Finite Element Method (FEM) is one of the easiest numerical techniques and hence most commonly used. Using FEM dynamic SSI effect can be simulated easily with desired precision. Nowadays, there are many software packages in the market for solving different problems using FEM. In this paper, a software named Abaqus (v.14.5) has been used to model and solve the above stated problem. Generally, to solve a SSI problem in Abaqus, some procedures have to be successively conducted. It is important to note that several important site response study were carried out by several researcher by using Abaqus. Yao et al.(Yao et al. 2019) successfully conducted site response by forming large-scale four-layered free-field model subjected to spatially varying seismic ground motions using Abaqus. In another research, Yao et al.(Yao et al. 2020) used Abaqus for simulating fully non-stationary

Table 1. Properties of the soils

Type of Soil	Mass Density (ρ) in kg/m^3	Young's Modulus (E) in N/m^2	Poisson's Ratio (ν)	Shear Wave Velocity (V_S) in m/s
Hard Soil	2300	1.99×10^9	0.2	600
Medium Soil	2000	6.5×10^8	0.32	350
Soft Soil	1500	9.7×10^7	0.43	150

Table 2. Properties of the constituents of the buildings

1.	**Grade of Concrete**		**M 25**
2.	**Mass Density (ρ) of Concrete**		2500 kg/m^3
3.	**Young's Modulus (E) of Concrete**		2.5×10^{10} N/m^2
4.	**Poisson's Ratio (ν) of Concrete**		0.15
6.	**Floor to Floor Height of the Building**		3 m
7.	**Depth of Footing**		2.5 m
8.	**Cross-sectional Area of the Columns**	**G+1 Building**	300 mm × 300 mm
		G+4 Building	400 mm × 400 mm
		G+9 Building	500 mm × 500 mm
9.	**Cross-sectional Area of the Beams**	**G+1 Building**	250 mm × 300 mm
		G+4 Building	250 mm × 400 mm
		G+9 Building	300 mm × 500 mm

spatially varying seismic motions by taking into account the nonlinear behavior of soil. Jin et al.(Jin et al. 2021) verified seismic response of flat ground and slope models using Abaqus and shake table test and found good agreement of numerical result with the experimental results. Seismic site response of layered saturated sand were performed by Nagula et al.(Nagula et al. 2021) by Abaqus and efficaciously verified with centrifuge test results.

In the first step geometries of different parts of the soil-structure model has ben conducted in the PART module. After that the materials and sections with desired properties have been formed and to the parts created before in the PROPERTIES module has been assigned. In the next step in ASSEMBLY module the whole soil-structure model combining all the parts have been suitably generated and type of analysis has been mentioned in the step module. Sequentially the sizes and properties of the elements of individual parts has been chosen as per requirement in the MESH module. After that appropriate boundary conditions of the model have been introduced in the LOAD module. The type of interaction (or, constraints) between the different components of the model has been indicated in the INTERACTION module. In the JOB module the job has been created and submitted for analysis. The output can be obtained VISUALIZATON module.

In this study, Infinite Soil, Soil Base, Soil Tetrahedron, Footing, Column and Beam, have been used to model the above stated soil-structure interaction problem. The plan dimensions of the soil base part (32.5 m × 32.5 m) has been considerd almost double compared to the plan dimensions of the structure (15 m × 15 m) so that its boundaries is not disturbed the response of the structure. The depth of the soil layer is 30 m and it is also kept higher than the depth of foundation ie 2.5 m. In order to fit the soil tetrahedron into it, a 22.5 m × 22.5 m × 5 m rectangular hollow has been developed at the centre of the soil base. The soil tetrahedron part actually acts as a bridge between the foundation and the soil base. This part also has a square shaped hollow where the dimensions of the hollow are equal as that of the foundation. The foundation has been positioned in its respective groove. The beams of length 5 m has been placed on top of each two adjacent columns. Homogeneous materials have been assigned as per the predefined properties. In according to that, the required sections for all the parts have been generated and have been allocated. Proper orientations have also been allocated to the beams and the columns. After creating all the parts and assigning all the material properties and section properties to them, they have been gathered in the right shape to obtain the complete soil-structure model. All the stress and displacement components under the input seismic motion have been achieved. It is to be mentioned that meshing is the most important part of the finite element method and the size of mesh plays an significant role in the calculation process. Though the finer mesh yields accurate solution, with the reduction in mesh size, the number of nodes and elements increases which requires more computer memory consumption and more computation time requirement. Therefore, an optimum mesh size has to be designated so that neither problem in accuracy of solution nor problem in computer memory and computation time arises. Keeping this in mind, the soil base and the infinite soil has been meshed using eight-noded linear brick elements having size 2.5 m × 2.5 m × 2.5 m, whereas the foundation has been meshed using eight-noded linear brick elements having size 0.625 m × 0.625 m × 0.625 m (Type C3D8). The soil tetrahedron has been suitably meshed using four-noded linear tetrahedron elements so that it can be linked to the soil base as well as to the footing. Infinite soil has been assumed as Linear Hexahedron element (CIN3D8). The beams and the columns have been meshed using two-noded linear elements of 1 m and 0.6 m length respectively.

In order to carry out the modal analysis, the whole model has been considered fixed at the base. Further, to incorporate this property, all the displacement and rotation components of the nodes present at the bottom of the model have been restricted to zero. Furthermore, to perform seismic analysis, only the displacement component of the bottom nodes along the direction of earthquake force has been released.

Finally, all the duplicate nodes have been merged to fix all the parts with one another and to get the complete model. Different views (Plan, Elevation and Isometric view) of the prepared models for the G+1, G+4 and G+9 buildings have been shown in Figure 1 to Figure 3.

In order to include the effect of damping in the soil-structure models, Rayleigh damping coefficients α and β have been evaluated for every model using Equation (1) and Equation (2) (Chowdhury & Dasgupta, 2003) having a damping ratio of 0.05. For computing the Rayleigh damping

Figure 1. Different views of the G+1 building

Figure 2. Different views of the G+4 building

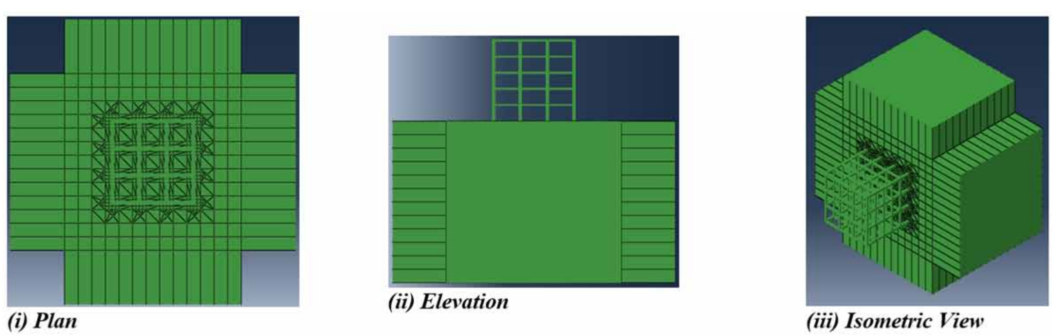

Figure 3. Different views of the G+9 building

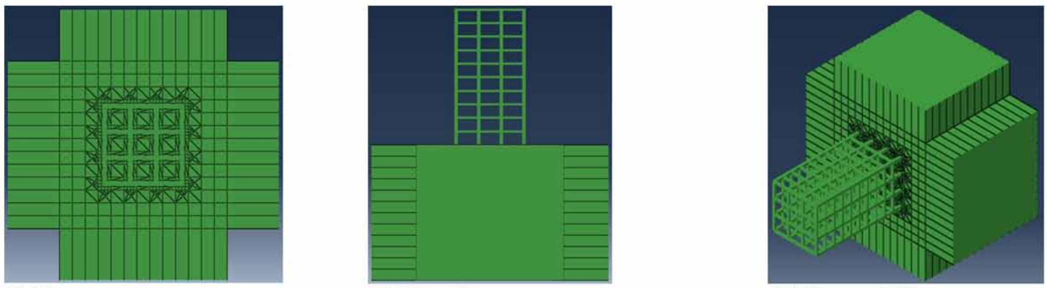

(i) Plan (ii) Elevation (iii) Isometric View

coefficients, first and fifth mode frequencies has been taken into account. Preparing all the models, dynamic analysis has been conducted to obtain the first mode and fifth mode frequencies.

$$\beta = \frac{2\xi_1\omega_1 - 2\xi_m\omega_m}{{\omega_1}^2 - {\omega_m}^2} \ldots \tag{1}$$

$$2\xi\omega_1 = \alpha + \beta{\omega_1}^2 \ldots \tag{2}$$

In Equation (1) and Equation (2), m denotes number of significant modes considered. It is to be noted that in the presnt study five nodes have been considered. ξ_1 signifies the damping ratio of the first mode, ξ_m signifies the damping ratio of the m-th mode (In this problem, $\xi_1 = \xi_m = \xi$), ω_1 denotes the frequency of the first mode, ω_m denotes the frequency of the m-th mode. In order to obtain the correct models, these Rayleigh damping coefficient values have been allotted to all the materials of the respective models.

4. INPUT MOTIONS AND THEIR PROPERTIES

To find out the effect of epicentre distance of an earthquake on dynamic soil-structure interaction phenomenon, all the developed models are subjected to a near-field earthquake as well as to a far-field one. Loma Prieta earthquake (1989) has been considered here as a representative of near-field earthquakes, while Denali earthquake, which occurred in 2002, represents the family of far-field earthquakes (https://peer.berkeley.edu/peer-strong-ground-motion-databases). Table 3 shows some general properties of the aforementioned earthquakes (i.e. Loma Prieta and Denali Earthquakes). It is to be noted that in near field seismic wave all types of frequency presents and in far field seismic wave only low frequency seismic wave presents.

In Figure 4, the acceleration time histories of these two earthquakes have been presented. In addition to that, for better understanding of the other properties of these earthquakes, acceleration response spectra and Fast Fourier Transform (FFT) have also been generated for both of them, which are displayed in Figure 5 and Figure 6 respectively.

5. DISPLACEMENT TIME HISTORIES OF ROOF AND BASE RESPONSES

After carrying out the entire analysis in Abaqus, the displacement time histories of both roof and base have been plotted in case of every model. These plots are presented in Figure 7 and Figure 8 respectively. Figure 7 and Figure 8 clearly signifies that the base response under the action of a particular earthquake differs mainly due to the variation in soil properties. In other words, when the

Table 3. General properties of the earthquakes

Earthquake Name	**Loma Prieta**	**Denali**
Year	1989	2002
Station Name	UCSC	Valdez - Valdez Dock Company
Earthquake Type	Near-Field	Far-Field
Epicentre Distance (R_{rup})	18.51 km	239.52 km
Mechanism	Reverse Oblique	Strike Slip
Magnitude	6.93	7.9
Recorded station V_{s30}	713.59 m/s	708.02 m/s
Spectral Ordinate	SRSS	SRSS
Scale Factor	1	1
Peak Ground Acceleration	0.311 g	0.009 g
Peak Ground Velocity	10.208 cm/s	1.77 cm/s
Peak Ground Displacement	4.054 cm	1.296 cm

Figure 4. Acceleration time histories of the earthquakes

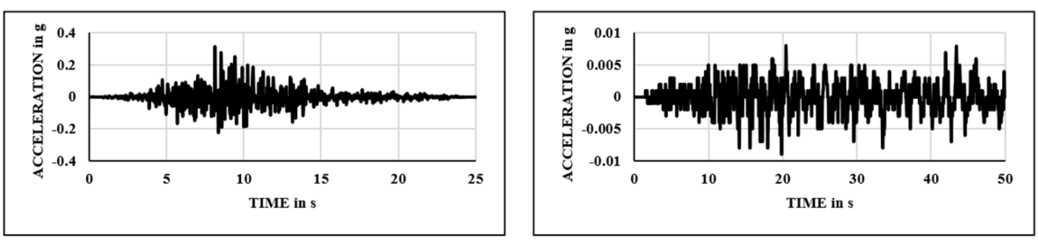

(i) Loma Prieta Earthquake *(ii) Denali Earthquake*

Figure 5. Acceleration response spectra of the earthquakes

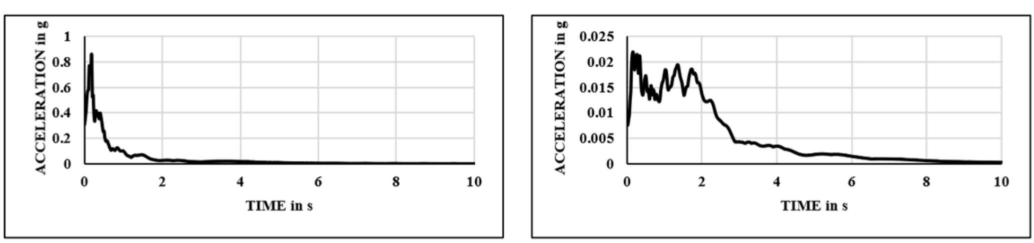

(i) Loma Prieta Earthquake *(ii) Denali Earthquake*

Figure 6. Fast Fourier transform (FFT) of the earthquakes

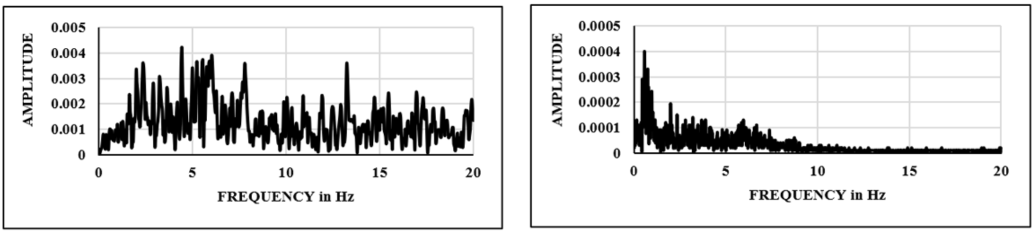

(i) Loma Prieta Earthquake *(ii) Denali Earthquake*

input motion and soil type are kept unchanged, no significant alteration in the base response is observed with the change in building height. It is also to be mentioned that for most cases, when a particular building is subjected to a certain earthquake, the roof drift has the highest value when the building is located on hard soil. On the contrary, for building resting on soft soil, roof displacement is the least. This is observed perhaps due to the higher flexibility effect of soft soil. However, when a G+9 building is subjected to a near-field earthquake, the maximum roof displacement is observed when it rests on medium type of soil. The reason behind this may be the higher value of spectral acceleration for medium soil, which acts on this building. Again, if all other parameters are kept identical, the roof drift of a G+9 building is the maximum and that of a G+1 building is the minimum. Further, the roof response of any building due to a far-field earthquake motion is always more than that due to a near-field earthquake excitation. This may be due to the presence of low frequency seismic waves in the far field ground motion.

6. MAXIMUM DISPLACEMENT PROFILES

The maximum displacements of all the floors for each model have been determined from the displacement time history data of the respective floor and these values are then plotted accordingly to generate the maximum displacement profile of every building. The plots thus obtained are shown in Figure 9. Figure 9 demonstates that the base response along with the roof response is maximum for hard soil and minimum for soft soil. This may be presence of damping in the soft soil. It is also to be noted that under the action of a far-field earthquake, the maximum displacements of the floors always increase monotonically with their heights. Again, when a near-field earthquake is subjected to a G+4 or G+9 building situated on hard or medium soil, the maximum displacements of the floors first decreases and then increases with the increase in height. This may be due to the presence of seismic waves having wide range of frequencies in the near-field earthquake excitation. In all other cases, the shape of the maximum displacement profile of the building strictly depends on the type of structure and soil.

7. FRAGILITY CURVES

Fragility analysis is an effective statistical method used for determining the vulnerability of a structure. By performing fragility analysis fragility curves can be developed, which are nothing but a graphical representation of change in probability of exceedance of Engineering Damage Parameter (EDP) at particular limit capacities (IO, LS and CP) with the variation of certain specific demand. The EDPs may be roof drift, percentage storey drift, energy dissipation etc. On the other hand, the demands may be Peak Ground Acceleration (PGA), Peak Ground Displacement (PGD), Spectral Acceleration for a specific time period etc. Again, Probabilistic Seismic Demand Model (PSDM) defines EDP as a function of Intensity Measure. Usually, it is represented by a curve indicating the alteration of percentage storey drift with respect to the change of PGA. PSDMs and fragility curves can be developed by LHS-Monte Carlo method and 2000 SAC/FEMA (American Society of Civil Engineers, 2000) method.

Cornell et al. (2002) (2002) has studied the probabilistic exceedance for seismic design along with limit capacity addressing the uncertainties in hazard, structural damage, and loss analysis. The relationship between probabilistic exceedance limit and seismic intensity is determined using NTHA. The equations for the EDP function and probabilistic exceedance limit are also developed. The framework, which provides the probabilistic basis for design recommendations, is obtained from the 2000 SAC/FEMA project (American Society of Civil Engineers, 2000).

Figure 7. Displacement time histories of roof responses of the buildings under Loma PRIETA and Denali earthquakes

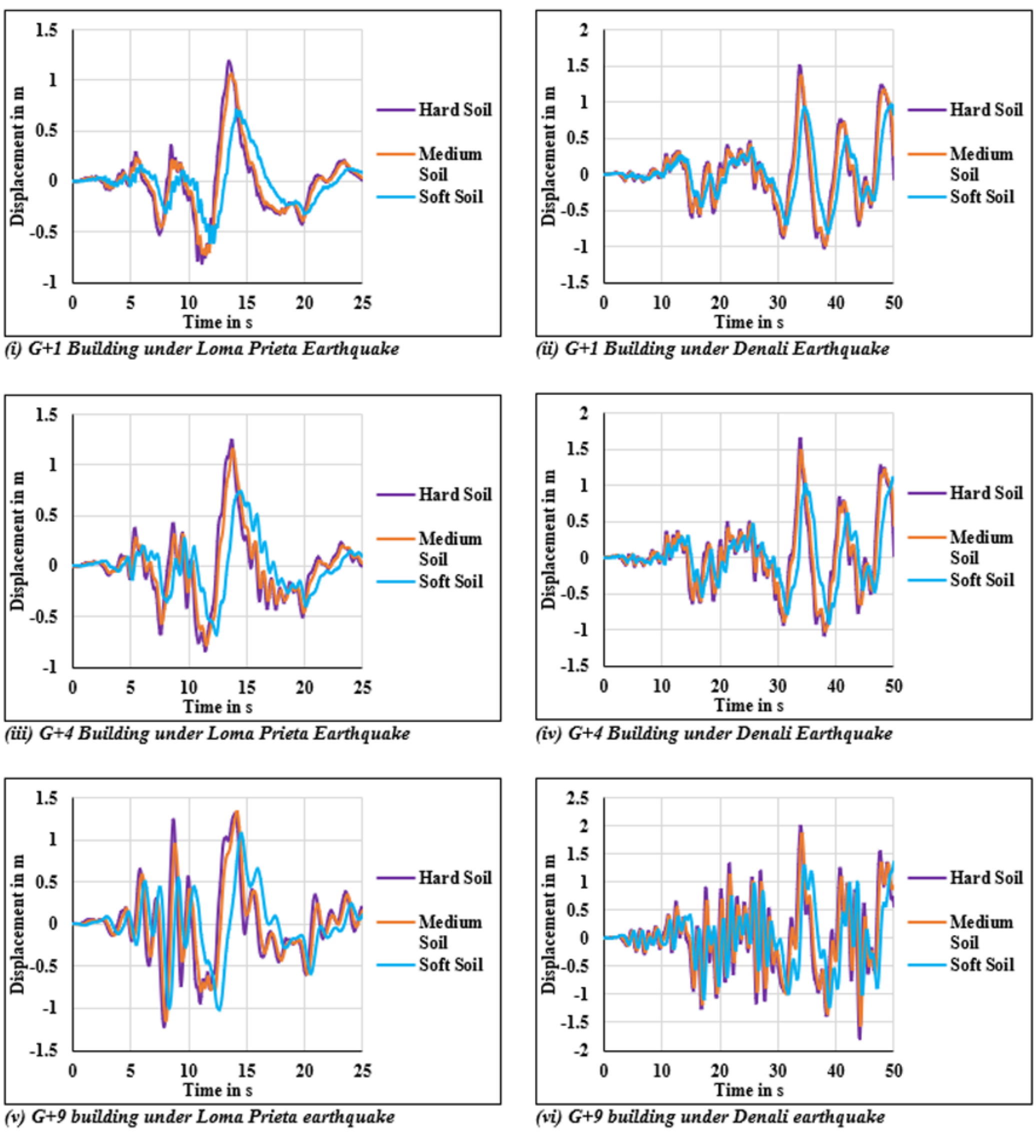

(i) G+1 Building under Loma Prieta Earthquake

(ii) G+1 Building under Denali Earthquake

(iii) G+4 Building under Loma Prieta Earthquake

(iv) G+4 Building under Denali Earthquake

(v) G+9 building under Loma Prieta earthquake

(vi) G+9 building under Denali earthquake

Figure 8. Displacement time histories of base responses of the buildings under Loma PRIETA and Denali earthquakes

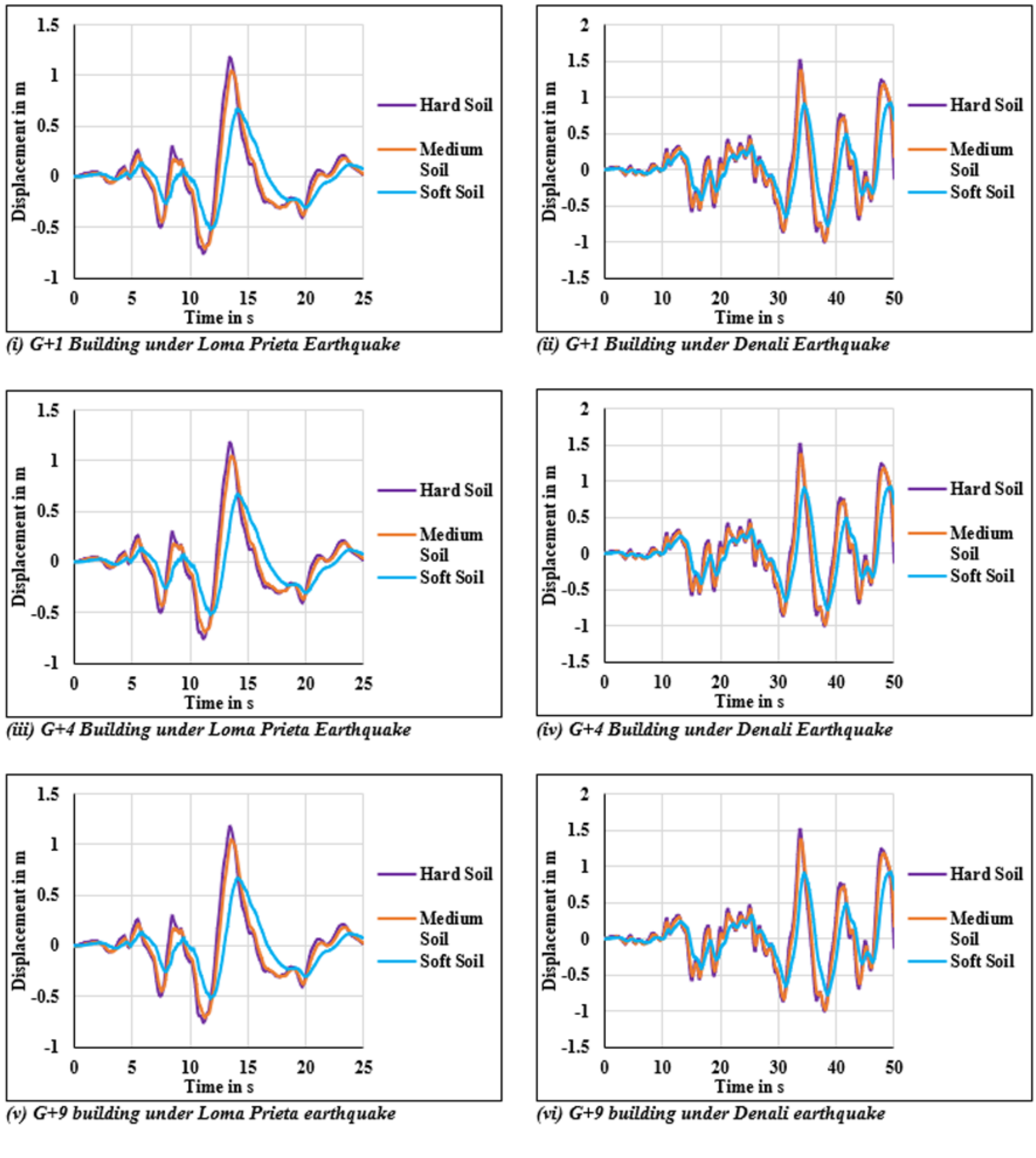

(i) G+1 Building under Loma Prieta Earthquake
(ii) G+1 Building under Denali Earthquake
(iii) G+4 Building under Loma Prieta Earthquake
(iv) G+4 Building under Denali Earthquake
(v) G+9 building under Loma Prieta earthquake
(vi) G+9 building under Denali earthquake

In this present methodology, a closed form expression has been used which comprises formula for evolving fragility curves. A fragility curve has been presented using a lot of discrete functions considering various uncertainties like uncertainties in modelling, material properties, rebar locations etc.

Celik and Ellingwood (2010) (2010) have presented the seismic fragility function by Equation (3).

Figure 9. Maximum displacement profiles of the buildings under Loma PRIETA and Denali earthquakes

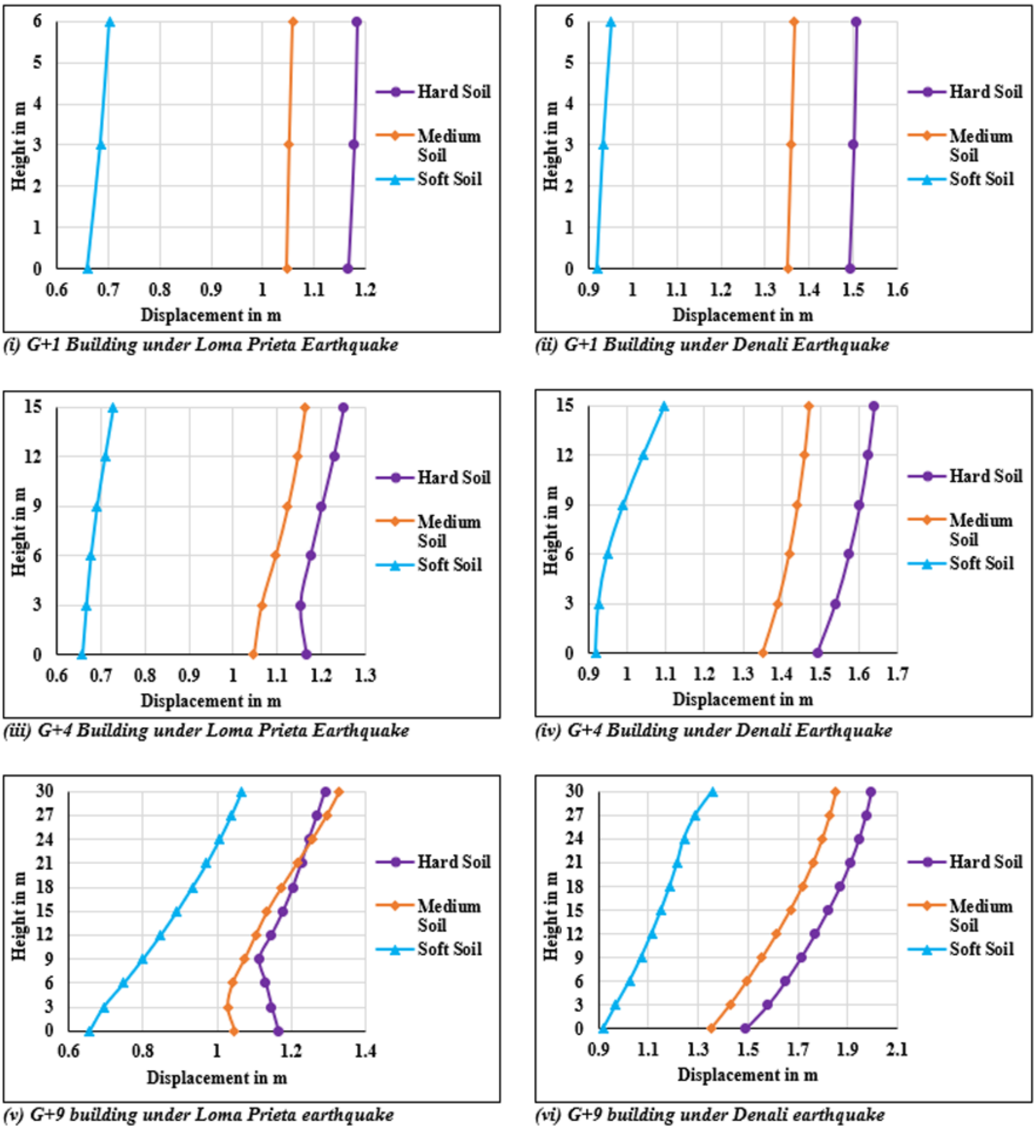

$$P\left(D \geq C \mid IM\right) = 1 - \varnothing\left(\frac{\ln \frac{S_C}{S_D}}{\sqrt{\beta_{D|IM}^2 + \beta_C^2 + \beta_M^2}}\right) \ldots \tag{3}$$

where, $\mathrm{P}\left(\mathrm{D} \geq \mathrm{C}\ |\mathrm{IM}\right)$ denotes the probability of exceedance of drift of ground storey for particular limit state capacities, D signifies the ground storey drift, C denotes the Drift capacity at the chosen limit state, $\beta_{D|IM}$ indicates the dispersion in the Intensity Measure (IM) like ground storey drifts at different PGA levels, β_C demonstrates the dispersion in capacities, β_M presents the dispersion in modelling. S_C can be expressed in terms of IM at particular limit state capacities such as IO, LS and CP. S_D is also known as EDP and can be expressed in a generalised form in terms of IM, which is shown in Equation (4).

$$EDP = a\left(IM\right)^{b} \ldots \tag{4}$$

where, a and b represents the regression coefficients of the PSDM. Thus, using Equation (4), Equation (3) can be rewritten as:

$$P\left(D \geq C \mid IM\right) = 1 - \varnothing\left(\frac{\ln S_c - \ln\left(a.IM^{b}\right)}{\sqrt{\beta_{D|IM}^{2} + \beta_{C}^{2} + \beta_{M}^{2}}}\right) \ldots \tag{5}$$

From NTHA, dispersion in the ground storey drifts at different PGA levels, $\beta_{D|IM}$, has been cmputed using Equation (6).

$$\beta_{D|IM} = \sqrt{\frac{\sum\left[\ln\left(d_i\right) - \ln\left(a.IM^{b}\right)\right]^{2}}{N-2}} \ldots \tag{6}$$

Now, uncertainty associate to the value for β_C depends on strength and other properties of the materials used, construction quality etc. For existing buildings, β_C depends on field investigation and the documents ie drawings and designing which are available for the verification of accuracy. In case of new buildings, it highly depends on how well the assumptions for designing the structure match with the actual construction process in the field. It is to be noted that the values of β_C with representative conditions have been recommended in ATC-58 (2012). In the present investigation, the value of β_C has been considered as 0.25 (Pragalath et al., 2016), where the building design has been completed to a level design development, construction quality is assured and limited quality inspection is anticipated. As per ATC-58 (2012), the total dispersion in modelling, β_M, can be computed as:

$$\beta_M = \sqrt{\beta_C^{2} + \beta_q^{2}} \ldots \tag{7}$$

β_q signifies that the hysteretic models may not accurately demostrates the behaviour of the structural components, even if the details of construction are precisely known. In this study, the value of β_q has been considered as 0.25 (Pragalath et al., 2016). The limiting value of ground storey drift in terms of intensity measure (IM) at a particular limit state capacity (IO, LS, CP) can be obtained from FEMA 356 (2000) (American Society of Civil Engineers, 2000) and IS-1893 (Part-1):2016 (IS, 2016). However, according to IS-1893 (Part-1): 2016 (IS, 2016), the maximum limit for inter-storey drift is 0.004 means 0.4%. In the present study PSDMs and fragility curves have been plotted following the 2000 SAC/FEMA method (American Society of Civil Engineers, 2000) considering Immediate Occupancy (IO), Life Safety (LS), Collapse Prevention (CP) and Indian Codal Limit. A sample PSDM curve has been shown in Figure 10, while the developed fragility curves are presented in Figure 11 to Figure 13. After analysing the PSDMs and fragility curves of the frame buildings resting on uniform soil, several important remarks can be drawn. The steep slope of the PSDM curve indicates the probability of exceeding the prescribed limit state (IO, LS, CP or Indian Codal Limit) under a specific earthquake intensity (in terms of PGA). From the fragility curves, it is observed that under a particular earthquake, the probability of exceeding Indian Codal Limit is the maximum and that of Collapse Prevention is the minimum. It is also to be mentioned that, for any type of soil and under a specific seismic excitation, the probability of exceedance of a certain limit state in case of a G+1 building is always minimum and that of a G+9 building is always maximum. In addition to that, when a G+1 building is subjected to a particular earthquake, it has the least probability of exceeding a limit state when it is situated on hard soil. On the contrary, it has the largest probability of exceeding a limit state when located on soft soil. Further, under the action of a particular seismic excitation, a G+4 building has the lowest probability of exceeding any limit state when it rests on the medium soil. However, it should be noted that in case a building is located on hard or medium soil, the probability of exceedance of a specific limit state for that soil-structure system is more when it is subjected to a near-field earthquake. On the other hand, if the building rests on soft soil, the probability of exceedance value of the soil-structure system will be greater under the influence of far-field earthquake.

8. RELIABILITY CURVES

Reliability of a structure is its ability to meet some specific requirements within a stipulated time period under the considered operating conditions. Mathematically, reliability can be expressed using Equation (8).

$$\mathrm{Re}\,liabilty = 1 - \mathrm{Pr}\,obability\,of\ Failure\ \ldots \qquad (8)$$

At a specific performance level, the probability of failure can be determined by convolving the fragility curve $\mathrm{F_R}\left(\mathrm{x}\right)$ with the derivative of the seismic hazard curve $\mathrm{G_A}\left(\mathrm{x}\right)$. It is sometimes assumed that this conditional probability follows a lognormal probability distribution (Song & Ellingwood, 1999). Mathematically, the probability of failure (i.e. exceeding any limit state) can be expressed using Equation (9).

Figure 10. PSDM for roof of G+1 building on hard soil under Loma PRIETA earthquake

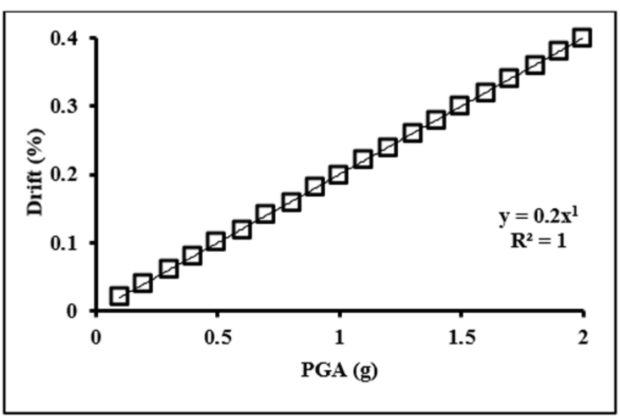

Figure 11. Fragility curves of roof when buildings rest on hard soil under Loma PRIETA and Denali earthquakes

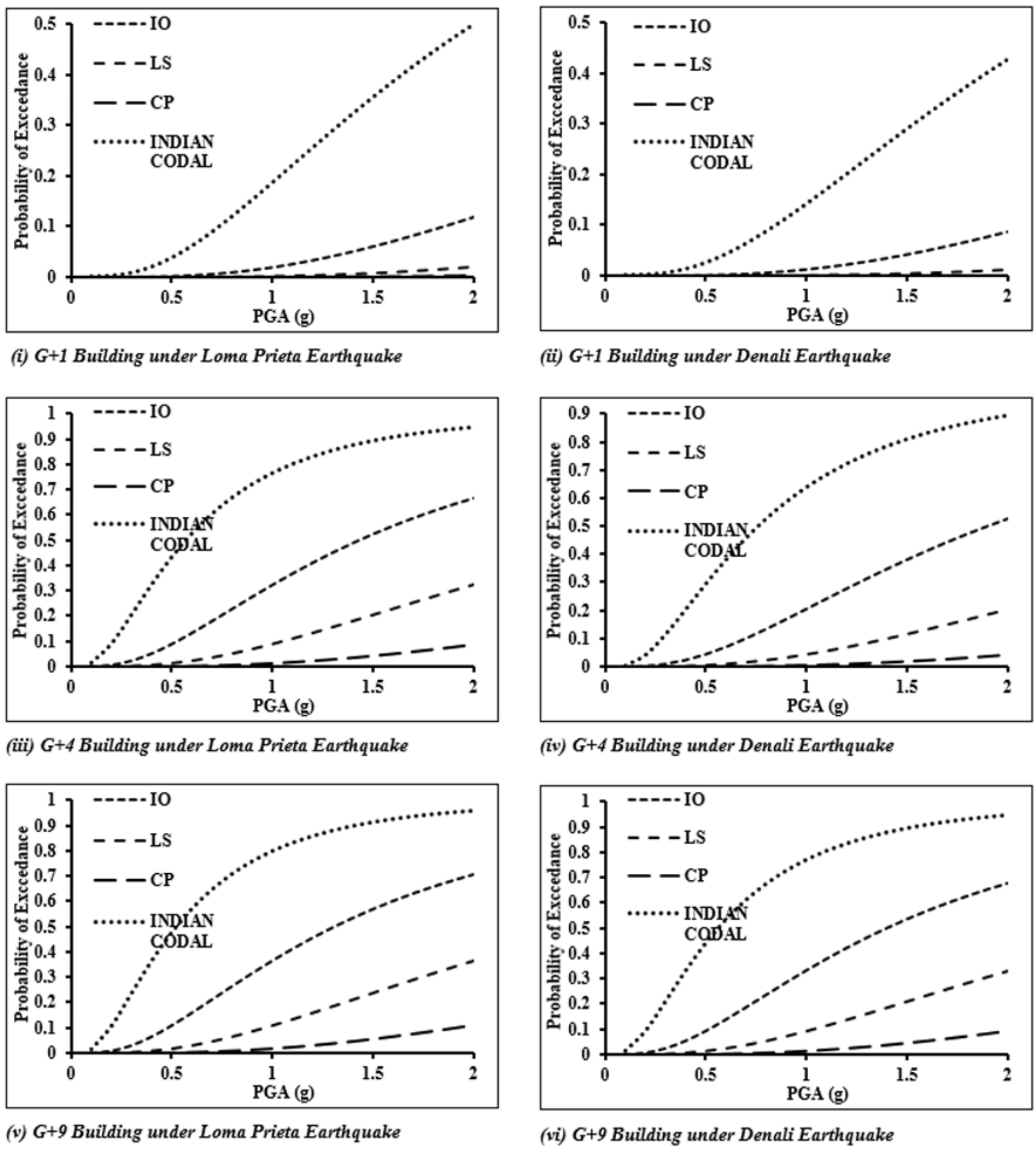

$$P\left[LS\right] = \int F_R\left(x\right)\frac{dG_A\left(x\right)}{dx}dx \ldots \tag{9}$$

Figure 14 shows the nature of fragility-hazard interface, as illustrated by Ellingwood (2001).

In Figure 14, $\mathrm{F_R}\left(\mathrm{x}\right)$ and $\frac{\mathrm{dG_A}\left(\mathrm{x}\right)}{\mathrm{dx}}$ are the two key parameters from which probability distribution P[LS] can be established. To determine the performance of each soil-structure system, Reliability Index (RI) has been computed which is a direct measure of the safety margin. According to Hassofer

Figure 12. Fragility curves of roof when buildings rest on medium soil under Loma PRIETA and Denali earthquakes

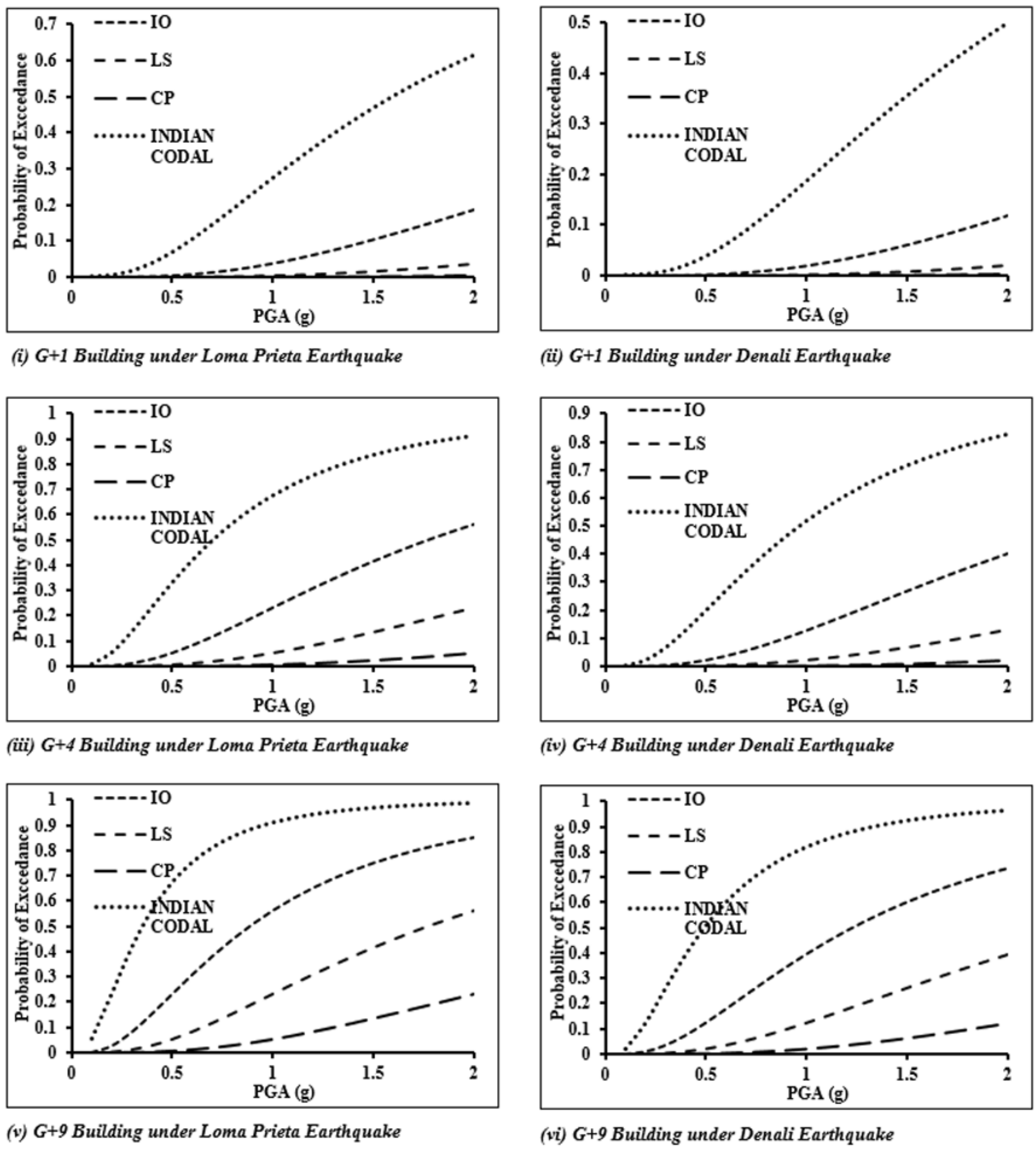

and Lind (1974), RI $\left(\beta_{pf}\right)$ is the shortest distance between the origin and the Limit State Function (LSF) in a standard normal variable space. RI $\left(\beta_{pf}\right)$ corresponding to a specific probability of failure at a certain performance limit can be computed using Equation (10).

$$\beta_{pf} = -\varnothing^{-1}\left(P\left[LS\right]\right)\ldots \tag{10}$$

where, Æ () denotes the standard normal distribution.

Figure 13. Fragility curves of roof when buildings rest on soft soil under Loma PRIETA and Denali earthquakes

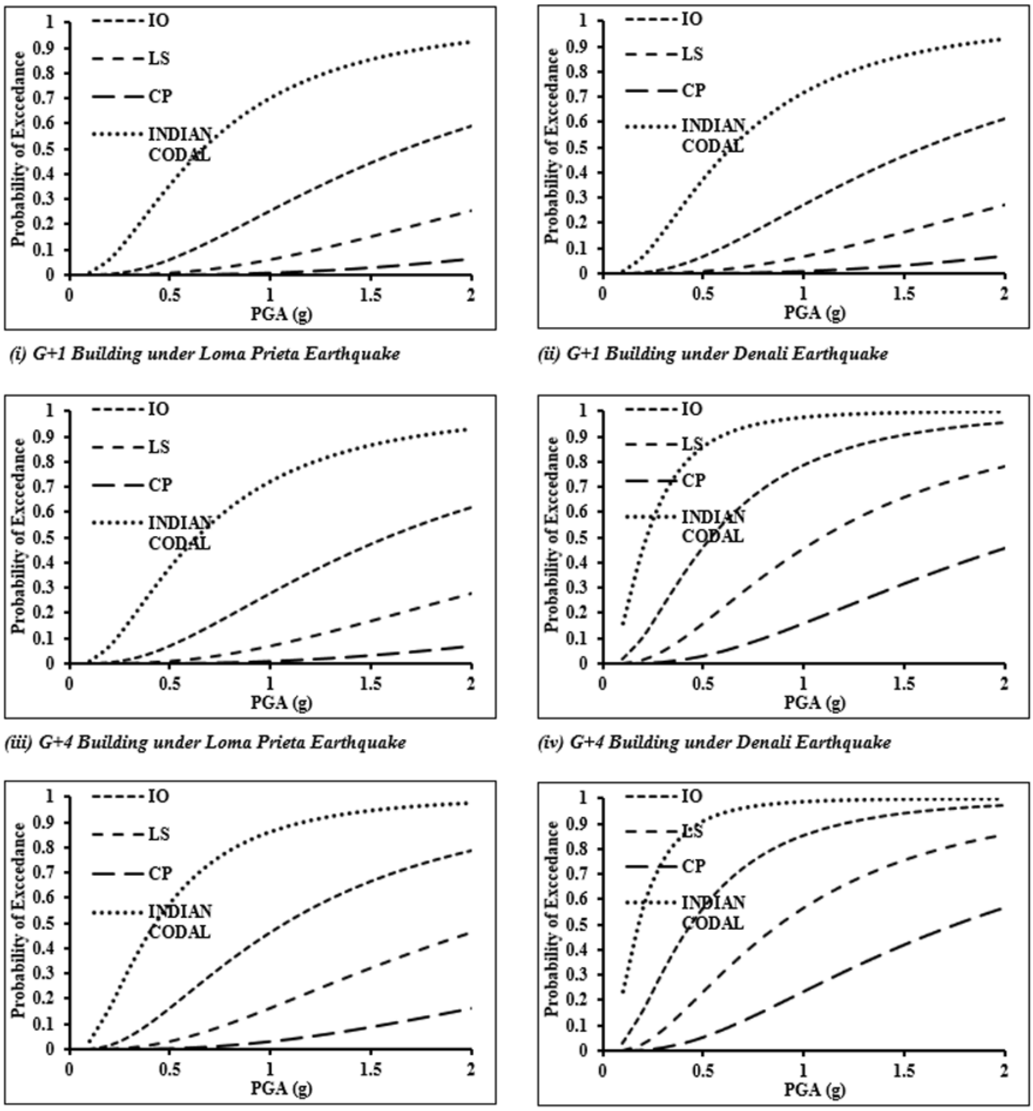

(i) G+1 Building under Loma Prieta Earthquake

(ii) G+1 Building under Denali Earthquake

(iii) G+4 Building under Loma Prieta Earthquake

(iv) G+4 Building under Denali Earthquake

(v) G+9 Building under Loma Prieta Earthquake

(vi) G+9 Building under Denali Earthquake

In Figure 15, the probability of failure has been indicated by the shaded area. In this figure, it is also clearly visible that Reliability Index (β_{pf}) is the shortest distance from the origin to the limit state function (LSF) in a standard normal variable space.

In this paper, total 18 sets of reliability curves (one set for each model) have been developed for the G+1, G+4 and G+9 frame buildings situated on three types of uniform soils (Hard Soil, Medium Soil and Soft Soil) in the Saltlake area which are subjected to a near-field (Loma prieta) and a far-field (Denali) seismic excitation. These curves are nothing but the combination of the fragility curves generated in the previous section of this paper along with the seismic hazard curve of Saltlake area (Nath et al., 2012) which has been presented in Figure 16. However, the reliability curves for all the models are shown in Figure 17 to Figure 19.

Figure 14. Fragility-hazard interface (ELLINGWOOD, 2001)

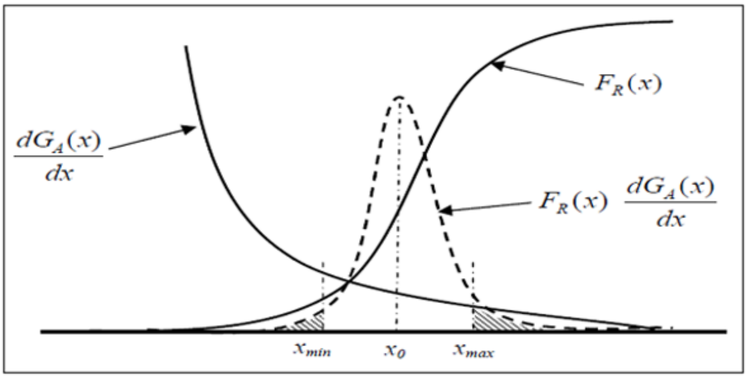

Figure 15. Probability density for limit-state (Ellingwood, 2001)

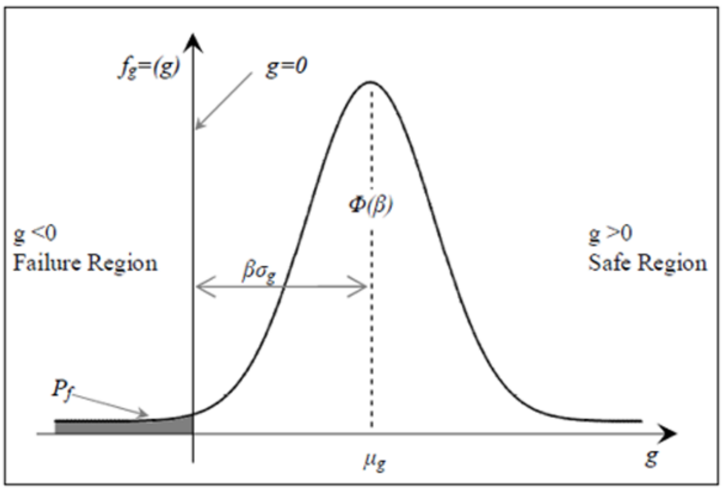

After analysing the reliability curves of the frame buildings situated on uniform soil, some important observations may be drawn. Firstly, for a specific type of soil and under a particular seismic excitation, the RI value of a G+1 building is always maximum and that of a G+9 building is always minimum. Again, if a G+1 building is subjected to a particular earthquake, it has the most RI value when it is situated on hard soil. On the other hand, it has the least RI value when it rests on soft soil. Further, under the action of a particular seismic excitation, a G+4 building has the highest RI value when it is located on medium soil. It is also to be noted that for a building resting on hard or medium soil, RI value of the soil-structure system is more when it is subjected to a far-field earthquake like Denali earthquake. On the contrary, if the building rests on soft soil, the RI value of the soil-structure system is greater when it experiences a near-field earthquake like Loma prieta earthquake.

9. CONCLUSION

In the present investigation SSI effect of different frame buildings situated over various uniform soils has been determined by nonlinear dynamic analysis using three-dimensional finite element method

Figure 16. Seismic hazard curve for Saltlake area (Nath, 2012)

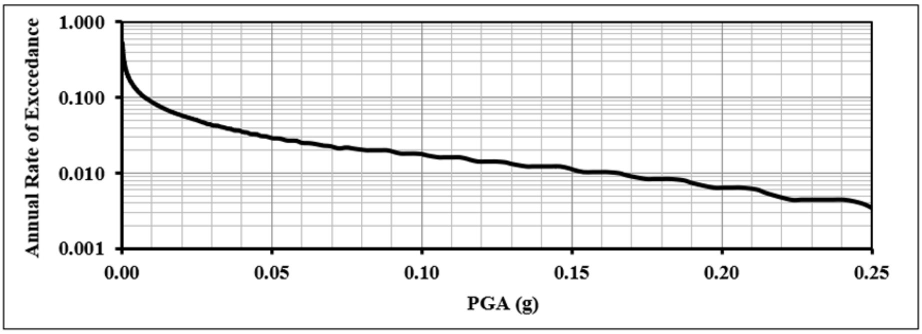

Figure 17. Reliability curves of roof when buildings rest on hard soil under Loma Prieta and Denali earthquakes

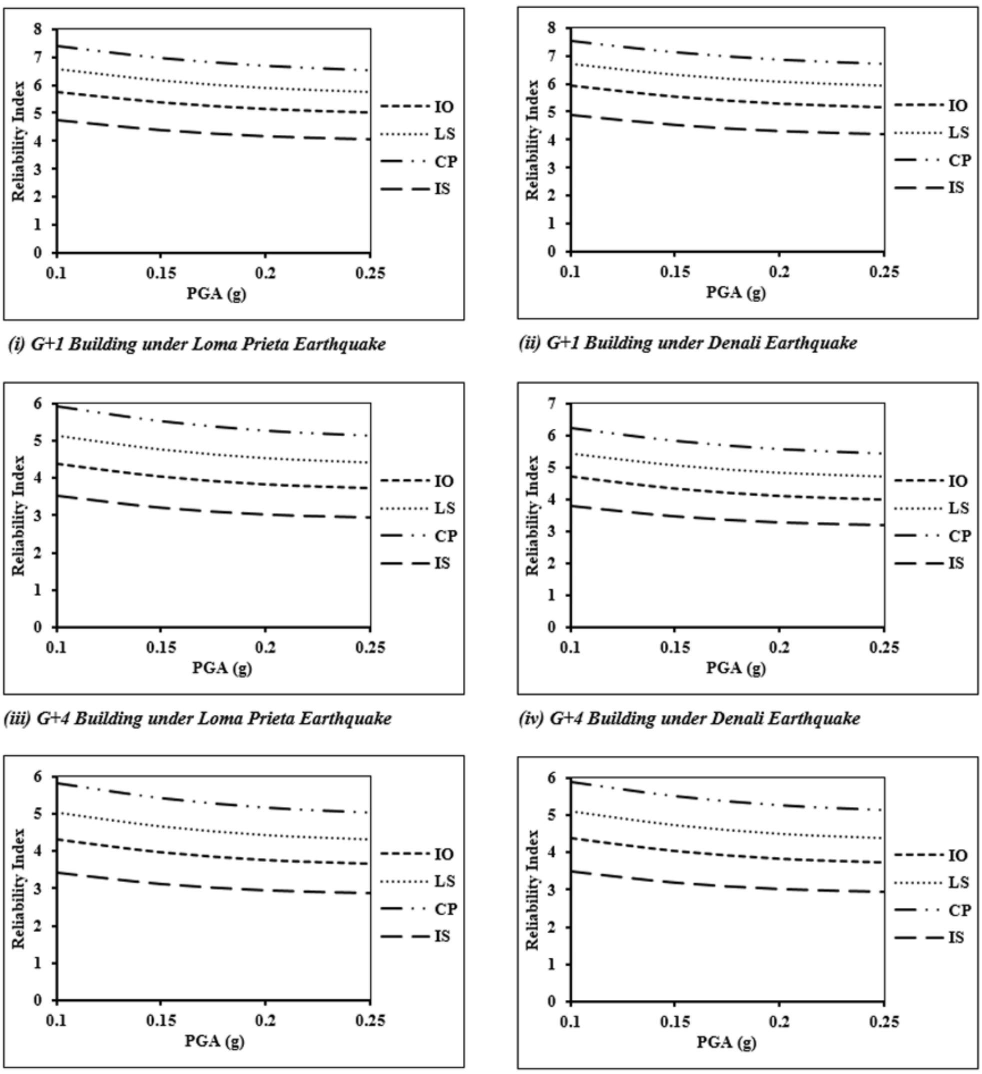

(i) G+1 Building under Loma Prieta Earthquake

(ii) G+1 Building under Denali Earthquake

(iii) G+4 Building under Loma Prieta Earthquake

(iv) G+4 Building under Denali Earthquake

(v) G+9 Building under Loma Prieta Earthquake

(vi) G+9 Building under Denali Earthquake

Figure 18. Reliability curves of roof when buildings rest on medium soil under Loma Prieta and Denali earthquakes

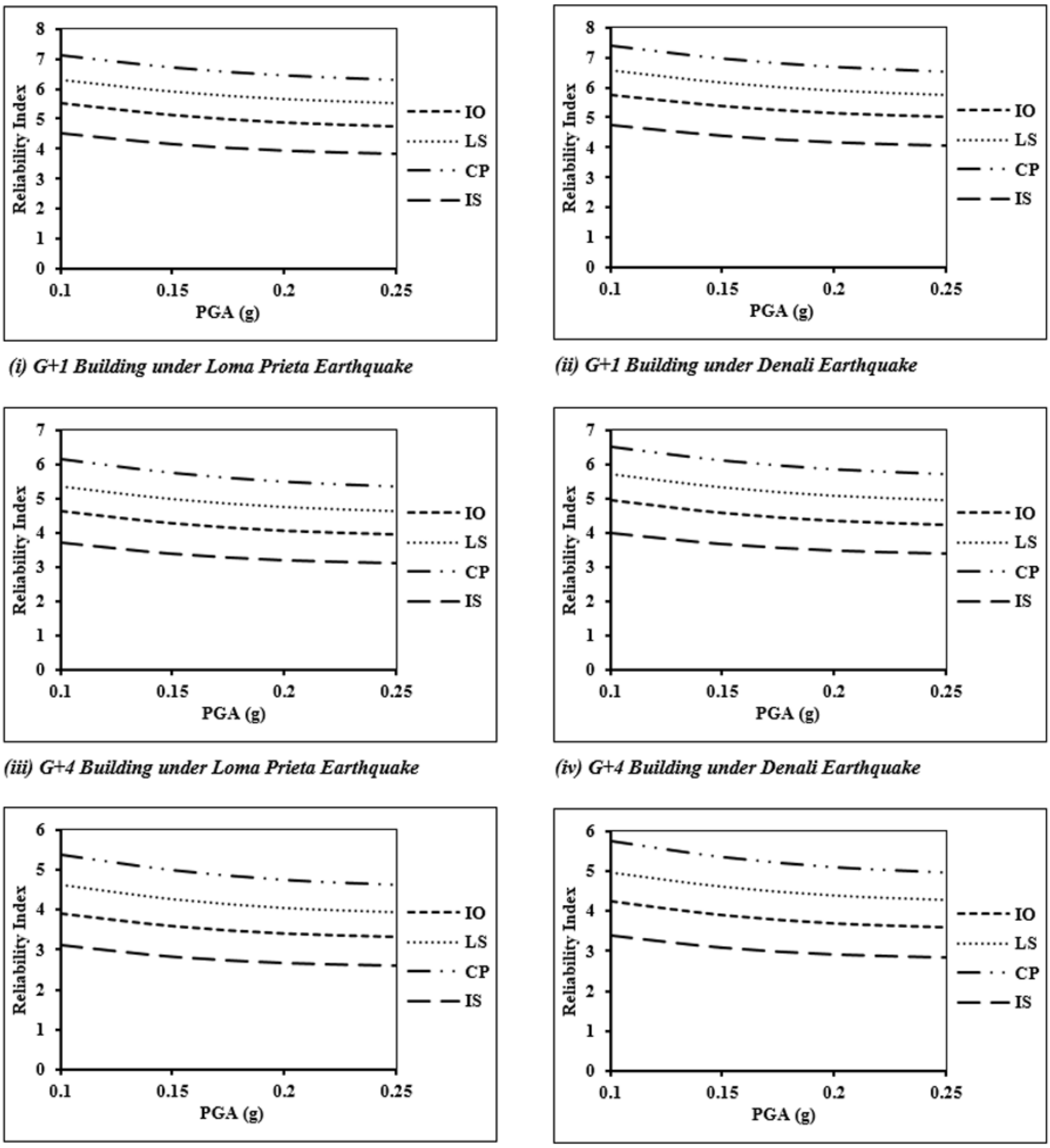

(i) G+1 Building under Loma Prieta Earthquake *(ii) G+1 Building under Denali Earthquake*

(iii) G+4 Building under Loma Prieta Earthquake *(iv) G+4 Building under Denali Earthquake*

(v) G+9 Building under Loma Prieta Earthquake *(vi) G+9 Building under Denali Earthquake*

software. Three types of uniform soils namely hard soil, medium soil and soft soil for low mid and high rise buildings (G+1, G+4 and G+9 storey) have been considered for the present analysis. The shear wave velocity of the three earthquakes are 600 m/s, 350m/s and 150 m/s respectively. The buildings under the above mentioned soil conditions have been subjected to monotonic increasing scaled Loma Prieta (1989) earthquake motion and Denali (2002) earthquake motion as near field and far field earthquake motions respectively. It is to be noted that epicentre distance of the two earthquakes are 18.51 km and 239.52 km respectively. The horizontal displacements and percentage drifts of all the storeys of the buildings have been determined and fragility curves have been generated. In addition to that, on the basis of the fragility curve and seismic hazard curve of a region, RI have also been

Figure 19. Reliability curves of roof when buildings rest on soft soil under Loma Prieta and Denali earthquakes

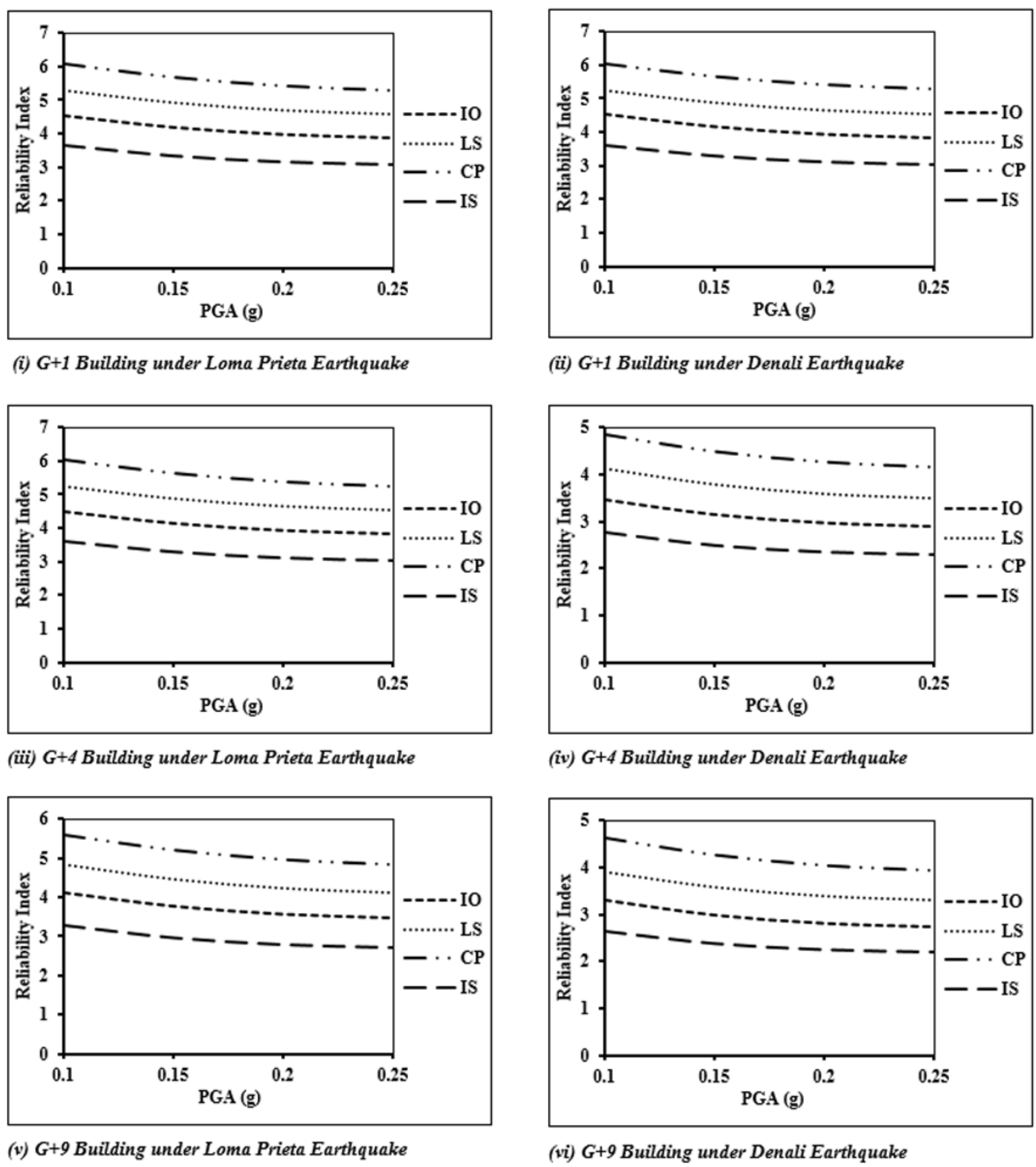

developed. It is to be noted that In Indian code (IS 1893-2016) the roof drift limit is mentioned 0.4%. However, in the present investigation in addition to Indian code permissible limit, Immediate Occupancy (IO), Life Safety (LS), Collapse Prevention (CP) were taken into account to generate the fragility curve and reliability index. Abacus 3D models have been prepared in with the considered non-linear soil parameters and then it is subjected to seismic input motions in terms of acceleration time history. Thus, it automatically considers the wave propagation effect through soil media, which is nothing but seismic site effects. But here the added advantage is the SSI consideration in the analysis.

Present study reveals that the base displacement along with the roof displacement is maximum for hard soil and minimum for soft soil for all the types of buildings under the two seismic motions.

This may be presence of high value of damping in the soft soil. Further, under the action of a far-field earthquake, the maximum displacements of the floors always increase uniformly with their heights. However, when a near-field earthquake is subjected to a mid to high rise buildings buildings situated on hard or medium soil, the maximum displacements of the floors first decreases and then increases with the increase in height. Possibly this is due to the presence of all type of frequency wave in the near-field earthquake excitation. Moreover, in all other cases, the shape of the maximum displacement profile of the buildings firmly depends on the type of structure and soil.

The fragility curves depicts that under a particular earthquake, the probability of exceeding Indian Codal Limit(0.4% roof drift) is the maximum and for Collapse Prevention (3% roof drift) it is minimum. It is important to note that, for any type of soil condition under a specific seismic excitation, the probability of exceedance of a certain limit state in case of a low storied (G+1 storied) buildings is always smallest and that of a high rise building is always largest. Further, when a lowere storied (G+1 storied) building is situated on hard soil and exposed to a particular seismic event, it has the least probability of exceeding a limit state. Furthermore, it has the largest probability of exceeding a limit state when located on soft soil. It is also to be observed that, under the action of a particular seismic excitation, buildings has the lowest probability of exceeding any limit state when it rests on the medium soil. However, it should be noted that in case a building is located on hard or medium soil, the probability of exceedance of a specific limit state for that soil-structure system is more when it is subjected to a near-field earthquake. On the other hand, if the building rests on soft soil, the probability of exceedance value of the soil-structure system will be greater under the influence of far-field earthquake.

The reliability curves signifies that RI value for low rise building is lesser than the high rise buildings. Further, if a low rise building is subjected to a particular earthquake, it has the most RI value when it is situated on hard soil. Alternatively, it has the least RI value when it situated on soft soil. Further, under the action of a particular seismic excitation, a mid rise building has the highest RI value (greater than 6) when it is located on medium soil. It is also to be noted that for a building resting on hard or medium soil, RI value is more when it is subjected to a far-field earthquake. On the contrary, if the building situated on soft soil, the RI value of the soil-structure system is larger when it experiences a near-field earthquake.

The reliability of the result obtained can be verified qualitatively with relevant well known researches (Krammer 1996). Here base displacement along with the roof displacement is maximum for hard soil and minimum for soft soil for all the types of buildings under the two seismic motions may be presence of high value of damping in the soft soil. Further, as far-field seismic motion consist lower frequency seismic wave, the maximum displacements of the floors always increase uniformly with their heights. However, as near field seismic motion consist both low and high frequency seismic wave, mid to high rise buildings located on hard or medium soil, the maximum displacements of the floors first decreases and then increases with the increase in height.

It is to be mention that to carry out dynamic analysis using three-dimensional finite element method software incorporating SSI effect of different frame buildings is very much time consuming and it requires lot of memory of computer. Thus, in the present study only soil damping effect has been considered. However, site effect due to presence of different layer should be taken into account in future study as effect of soil layers plays an important role in ground motion characteristics ((Krammer 1996)(Shiuly, Kumar, and Narayan 2014) (Roy et al. 2018)(Pandey et al. 2021)(Pandey and Jakka 2022). Further, in the present investigation effect of reinforcement of structure has not taken into account. However, the present study is very much effective to understand the behavior of buildings considering SSI under near and far field earthquake at different soil condition. Further, fragility and reliability curve enhance the knowledge of damage probability of different buildings with above mention condition.It is important to mentioned that the study is not region specific and it can be conducted for buildings subjected near field and far field earthquake situated any region which may consists soft, medium or hard type of soil.

CONFLICTS OF INTEREST

We wish to confirm that there are no known conflicts of interest associated with this publication and there has been no significant financial support for this work that could have influenced its outcome.

FUNDING STATEMENT

No funding was received for this work.

PROCESS DATES:

Received: June 3, 2021, Revision: April 22, 2022, Accepted: May 14, 2022

CORRESPONDING AUTHOR:

Correspondence should be addressed to Amit Shiuly; amit.shiuly@yahoo.in

REFERENCES

American Society of Civil Engineers. (2000). NEHRP Guidelines for Prestandard and Commentary for the Seismic Rehabilitation of Buildings. Author.

Anand, Mightraj, & Prince Arulraj. (2010). *Seismic Behaviour of RCC Shear Wall Under Different Soil Conditions*. Academic Press.

ATC. (2012). *ATC-58, Seismic Performance Assessment of Buildings* (vol. 1). ATC.

Azharhoosh & Amiri. (2010). *Elastic Response of Soil-Structure Systems Subjected to Near-Fault Rupture Directivity Pulses.* Academic Press.

Boominathan, A., & Krishna Kumar, S. (2010, January). A Site Specific Study on Evaluation of Design Ground Motion Parameters. *International Journal of Geotechnical Earthquake Engineering*, *1*(1), 1–24. doi:10.4018/jgee.2010090801

Borele, S. V. (2015). Damage Assessment of Structural System Using Fragility Curves. *J. Civ. Eng. Environ. Technol.*, *2*, 72–76.

Celik, O. C., & Ellingwood, B. R. (2010). Seismic Fragilities for Non-ductile Reinforced Concrete Frames – Role of Aleatoric and Epistemic Uncertainties. *Structural Safety*, *32*(1), 1–12. doi:10.1016/j.strusafe.2009.04.003

Chowdhury & Dasgupta. (2003). Computation of Rayleigh Damping Coefficients for Large Systems. *Electron. J. Geotech. Eng.*, *8C*.

Collins, K. R., Wen, Y. K., & Foutch, D. A. (1996). Dual-level Seismic Design: A Reliability Based Methodology. *Earthquake Engineering & Structural Dynamics*, *25*(12), 1433–1467. doi:10.1002/(SICI)1096-9845(199612)25:12<1433::AID-EQE629>3.0.CO;2-M

Cornell, C. A., Jalayer, F., Hamburger, R. O., & Foutch, D. A. (2002). The Probabilistic Basis for the 2000 SAC/FEMA Steel Moment Frame Guidelines. *Journal of Structural Engineering*, *128*(4), 526–533. doi:10.1061/(ASCE)0733-9445(2002)128:4(526)

Davoodi, Sadjadi, Goljahani, & Kamalian. (2012). *Effects of Near-Field and Far-Field Earthquakes on Seismc Response of SDOF System Considering Soil Structure Interaction*. Academic Press.

Ellingwood, B. R. (2001). Earthquake Risk Assessment of Building Structures. *Reliability Engineering & System Safety*, *74*(3), 251–262. doi:10.1016/S0951-8320(01)00105-3

Gaikwad, M. V., Ghogare, R. B., & Vageesha, S. M. (2015). Finite Element Analysis of Frame with Soil Structure Interaction. *International Journal of Research in Engineering and Technology*, *4*(1), 91–95. doi:10.15623/ijret.2015.0401017

García. (2008). *Soil Structure Interaction in the Analysis and Seismic Design of Reinforced Concrete Frame Buildings.* Academic Press.

Gelagoti, F., Kourkoulis, R., Anastasopoulos, I., & Gazetas, G. (2012). Rocking-isolated Frame Structures: Margins of Safety against Toppling Collapse and Simplified Design Approach. *Soil Dynamics and Earthquake Engineering*, *32*(1), 87–102. doi:10.1016/j.soildyn.2011.08.008

Ghannad. (2008). *Effects of Soil-Structure Interaction on Response of Structures Subjected to Near-Fault Earthquake Records*. Academic Press.

Guneyisi, E. M., & Altay, G. (2008). Seismic Fragility Assessment of Effectiveness of Viscous Dampers in R/C Buildings under Scenario Earthquakes. *Structural Safety*, *30*(5), 461–480. doi:10.1016/j.strusafe.2007.06.001

Harichane, Z., Guellil, M. E., & Gadouri, H. (2018, January). Benefits of Probabilistic Soil-Foundation-Structure Interaction Analysis. *International Journal of Geotechnical Earthquake Engineering*, *9*(1), 42–64. doi:10.4018/IJGEE.2018010103

Hasofer, A. M., & Lind, N. (1974). An Exact and Invariant First Order Reliability Format. *Journal of Engineering Mechanics*, *100*(1).

IS. (2016). *1893 (Part-1)*. Criteria for Earthquake Resistant Design of Structures - General Provisions and Buildings. IS.

Karthika, A. P., & Gayathri, V. (2018). Literature Review on Effect of Soil Structure Interaction on Dynamic Behaviour of Buildings. *Int. Res. J. Eng. Technol.*, *5*(4), 2522–2525.

Kuladeepu, M. N., Narayana, G., & Narendra, B. K. (2015). Soil Structure Interaction Effect on Dynamic Behavior of 3D Building Frames with Raft Footing. *International Journal of Research in Engineering and Technology*, *4*(7), 87–91. doi:10.15623/ijret.2015.0407014

Kumar, S. S., Dey, A., & Krishna, A. M. (2018, January). Importance of Site-Specific Dynamic Soil Properties for Seismic Ground Response Studies. *International Journal of Geotechnical Earthquake Engineering*, *9*(1), 78–98. doi:10.4018/IJGEE.2018010105

Kumar, S. S., & Krishna, A. M. (2013, January). Seismic Ground Response Analysis of Some Typical Sites of Guwahati City. *International Journal of Geotechnical Earthquake Engineering*, *4*(1), 83–101. doi:10.4018/jgee.2013010106

Matinmanesh & Asheghabadi. (2011). *Seismic Analysis on Soil-Structure Interaction of Buildings over Sandy Soil.* Academic Press.

Minasidis, G., Hatzigeorgiou, G. D., & Beskos, D. E. (2014). SSI in Steel Frames Subjected to Near-Fault Earthquakes. *Soil Dynamics and Earthquake Engineering*, *66*, 56–68. doi:10.1016/j.soildyn.2014.06.030

23. Mosalam, K. M., Ayala, G., White, R. N., & Roth, C. (1997). Seismic Fragility of LRC Frames with and without Masonry Infill Walls. *Journal of Earthquake Engineering*, *1*(4), 693–720. doi:10.1080/13632469708962384

Nabilah, A. B., Koh, C. G., Safiee, N. A., & Daud, N. N. N. (2019, January). Effect of Flexible Soil in Seismic Hazard Assessment for Structural Design in Kuala Lumpur. *International Journal of Geotechnical Earthquake Engineering*, *10*(1), 30–42. doi:10.4018/IJGEE.2019010103

Nath, Adhikari, Maiti, Devaraj, Srivastava, & Mohapatra. (2012). Earthquake Scenario in West Bengal with Emphasis on Seismic Hazard Microzonation of the City of Kolkata. *J. Dep. Geol. Geophys. Indian Inst. Technol. Kharagpur*.

Pragalath, D. C. H., Bhosale, A., Davis, P. R., & Sarkar, P. (2016). Multiplication Factor for Open Ground Storey Buildings – A Reliability Based Evaluation. *Earthquake Engineering and Engineering Vibration*, *15*(2), 283–295. doi:10.1007/s11803-016-0322-4

Priyanka, R. M. J., Anand, N., & Justin, S. (2012). Studies on Soil Structure Interaction of Multi Storeyed Buildings with Rigid and Flexible Foundation. *International Journal of Emerging Technology and Advanced Engineering*, *2*(12), 111–118.

Shiuly, A., Sahu, R. B., & Mandal, S. (2014, January). Effect of Soil on Ground Motion Amplification of Kolkata City. *International Journal of Geotechnical Earthquake Engineering*, *5*(1), 1–20. doi:10.4018/ijgee.2014010101

Singhal, A., & Kiremidjian, A. S. (1996). Method for Probabilistic Evaluation of Seismic Structural Damage. *Journal of Structural Engineering*, *122*(12), 1459–1467. doi:10.1061/(ASCE)0733-9445(1996)122:12(1459)

Sitharam, T. G., & Vipin, K. S. (2010, January). Evaluation of Peak Ground Acceleration and Response Spectra Considering the Local Site Effects. *International Journal of Geotechnical Earthquake Engineering*, *1*(1), 25–41. doi:10.4018/jgee.2010090802

Song, J., & Ellingwood, B. R. (1999). Seismic Reliability of Special Moment Steel Frames with Welded Connections: I and II. *Journal of Structural Engineering*, *125*(4), 357–372. doi:10.1061/(ASCE)0733-9445(1999)125:4(357)

Stewart, J. P., Fenves, G. L., & Seed, R. B. (1999). Seismic Soil-Structure Interaction in Buildings: Analytical aspects. *Journal of Geotechnical and Geoenvironmental Engineering*, *125*(1), 26–37. doi:10.1061/(ASCE)1090-0241(1999)125:1(26)

Vazurkar, U. Y., & Chaudhari, D. J. (2016). Development of Fragility Curves for RC Buildings. *International Journal of Engine Research*, *5*, 591–594.

Wen, Y. K. (2001). Reliability and Performance-Based Design. *Structural Safety*, *23*(4), 407–428. doi:10.1016/S0167-4730(02)00011-5

Zhang & Tang. (2008). *Dimensional Analysis of Linear Soil-Foundation-Structure System Subjected to Near-Fault Ground Motions*. Academic Press.

Amit Shiuly passed B.E. from Jadavpur University in civil engineering and passed M.Tech in Earthquake Engineering from IIT Roorkee. He has done PhD in Civil Engineering Department, Jadavpur University. He is now Assistant Professor in Civil Engineering department of Jadavpur University.